Two-Photon Responsive Metal−Organic Framework

Jiancan Yu,[†,∥] Yuanjing Cui,[†,∥] Chuan-De Wu,[‡] Yu Yang,[†] Banglin Chen,*[,†,§] and Guodong Qian*[,†]

[†]State Key Laboratory of Silicon Materials, Cyrus Tang Center for Sensor Materials and Applications, School of Materials Science and Engineering, and [‡]Department of Chemistry, Zhejiang University, Hangzhou 310027, China

[§]Department of Chemistry, University of Texas at San Antonio, San Antonio, Texas 78249-0698, United States

Ⓢ Supporting Information

ABSTRACT: Two-photon processing presents a facile means to tailor the properties of materials in three-dimensions. A two-photon responsive metal−organic framework (MOF) has been realized through the incorporation of a photoactive linker into a MOF via a multivariate strategy. The resulting MOF exhibits a significant one-photon and two-photon excited fluorescence change in response to UV light and infrared femtosecond laser, enabling spatial modulation of the fluorescence property of the MOF. It thus demonstrates the capacity of two-photon patterning and imaging inside the crystal, and the formation of three-dimensional two-photon excited fluorescent structure in a high resolution.

M etal−organic frameworks (MOFs)[1,2] have been intensively explored for gas storage/separation,[3,4] catalysis,[5,6] chemical sensors,[7−9] electronics,[10] photonics,[11,12] ion conduction,[13−15] and as the precursors for the construction of porous carbon/metal oxide.[16] Their broad applications rely on their chemical and structural diversity, flexibility, and rational designability. Light responsive MOFs, whose chemical and structural changes can be controlled merely by mild condition-light irradiation, have shown intriguing properties and thus recently received great interest.[17−28] For example, light can induce configuration transformations of the linkers/guests, thus to tune the pores of MOFs and enhance their gas separation performances.[18−21] Photochemical reactions can also provide an alternative way to introduce functional groups/moieties and thus to develop smart MOFs with switchable optical absorption and fluorescence properties.[21−25] Because the light triggers the reactions in a one-photon process in these examined systems, we were not able to develop their spatial selectivity: the photochemical responses take place either on the surfaces or in the whole crystals of MOFs. It is essential to engineer the properties of MOFs using the light or laser in three-dimensional (3D) structure, which would create functional patterns inside the MOF crystals and find applications in chemical sensors, optical switches, data storage, and circuits.[29,30]

The task of manipulating the properties of MOFs in 3D can be realized by the usage of nonlinear optical effects, in particular through the multiphoton absorption. This is because such nonlinear optical processing has the advantages such as tight focus and deep penetration over linear absorption effects[31−34] and therefore can initiate reactions in the defined focal regions of laser within the bulky materials.[35−37] However, very rare multiple-photon responsive MOFs have been developed so far.[30,38,39] Here we report the first two-photon responsive MOF exhibiting two-photon excited fluorescence change. A photo-active zwitterionic pyridinium linker has been introduced into a MOF through the developed multivariate (MTV) strategy.[40] Because the linker exhibits two-photon absorption induced reaction, we take advantage of the two-photon process to spatially initiate the chemical reactions and engineer the two-photon excited fluorescence property of MOF crystal in the 3D structure, as schematically shown in Figure 1, leading to the 3D two-photon patterning and fluorescence imaging.

As previous reported, pyridinium salts display addition[41] and oxidation reactions under the irradiation of UV light[41] and show relatively large two-photon absorption cross-section;[42] we
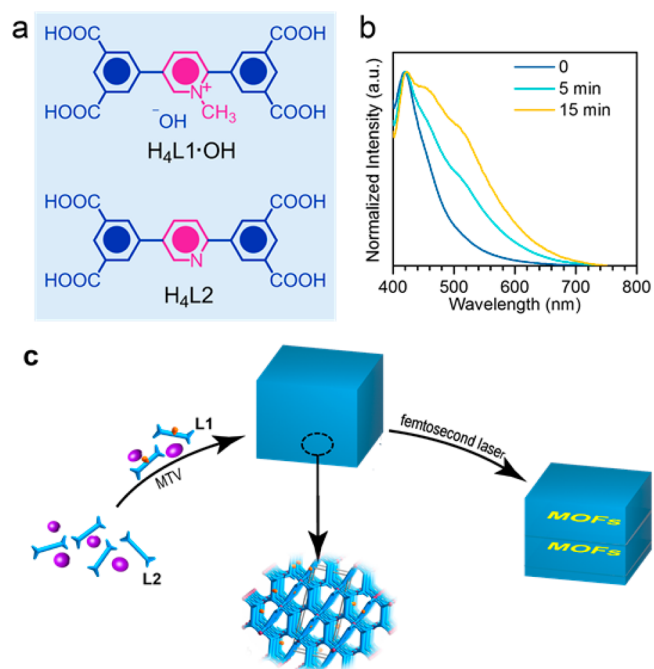

Figure 1. (a) Zwitterionic and neutral tetracarboxylate linkers for the construction of two-photon responsive MOFs. (b) Fluorescence spectra evolution of $H_4L1\cdot OH$ upon exposure to UV light at 365 nm. (c) Schematic illustration of the assembly of L1 incorporated MOF **ZJU-56−0.20** via a multivariate approach and femtosecond laser writing inside the MOF single crystal through a two-photon process.

thus designed and synthesized a zwitterionic pyridinium molecule, 2,5-bis(3,5-dicarboxyphenyl)-1-methylpyridinium hydroxide (H$_4$L1·OH, Figures 1a and S1), as a candidate linker to investigate the two-photon properties and process. Upon UV light irradiation at 365 nm, the fluorescence emission of the H$_4$L1·OH powder evolves gradually with a very broad emission band between 470 and 560 nm (Figure 1b). As expected, the appearance of new emission band suggests that the linker can be transformed into another fluorescent molecule upon light irradiation. In principle, it should be possible to build MOFs with light induced fluorescence change by making use of this linker.

As we were not able to get high crystalline MOFs from this organic linker (Figure S2), we thus applied the multivariate MOF approach to synthesize the light responsive MOFs.[40] Reaction of structurally similar linker 5,5′-(pyridine-2,5-diyl)-diisophthalic acid (H$_4$L2)[43] with Zn(NO$_3$)$_2$·6H$_2$O in a mixture solution of N,N-dimethylformamide (DMF) and acetonitrile readily afforded colorless crystals Zn(L2)$_2$2H$_2$O·solvents (ZJU-56). ZJU-56 crystallizes in the space group of $R\bar{3}m$ and adopts a 3D network of **fof** topology,[44] the same as its Cu-based counterpart.[43] When 20 mol % of H$_4$L1·OH was introduced to the reaction solution, the multivariate MOF crystals ZJU-56−0.20 of regular parallelepiped-like shape were obtained (Figure S3). The mixed MOF is isomorphic to ZJU-56 (Figure S4−6 and Table S1). As shown in Figure S7, ^{1}H NMR data of the digested MOF crystals show the characteristic peaks around 9.74, 9.10, 8.28, and 4.26 ppm attributed to the zwitterionic linker L1 in ZJU-56−0.20, and the content of L1 in the resulting MOF is determined to be 22%.

The single crystals of ZJU-56−0.20 (Figure S3) exhibit blue fluorescence with an emission peak around 450 nm from both the linkers (Figure 2a,b). When the single crystals of ZJU-56−0.20 were exposed to a UV lamp at a wavelength of 365 nm, the emission band around 450 nm decreases rapidly, while a new band centered at 550 nm emerges and increases gradually. After a period of 360 s, the blue fluorescence peak at 450 nm almost disappears and the fluorescence band around 540 nm dominates the whole spectrum, eventually resulting in the

Figure 2. (a) Fluorescent micrographs of a crystal ZJU-56−0.20 upon UV light irradiation. Left, initial; right, after 5 min; excitation wavelength, 365 nm. (b) Fluorescence spectra evolution. (c) Bright-field image of a single crystal of ZJU-56−0.20 and two selected regions that were exposed to a tunable laser at wavelengths of 710 and 900 nm, respectively. (d) Bright-field and fluorescence emerged images of this crystal after laser exposure. (e) Two-photon excited fluorescence spectra evolution of two regions that were experiencing laser irradiation. All scale bars, 100 μm.

fluorescence color change of the MOF from blue to yellow. It should be noted that the fluorescence change of the MOF in response to UV light irradiation is much faster than that of H$_4$L1·OH powder. As a reference, the single crystals of ZJU-56 exhibit no fluorescence color change after UV light illumination (Figure S8) because of the absence of the zwitterionic linker L1, indicating that the fluorescence change of ZJU-56−0.20 indeed originates from the photochemical reaction of the linker L1. ^{1}H NMR spectra of the linker L1 illuminated by UV laser show various proton peaks in the range of 4.5−7.5 ppm (Figure S9a), which are characteristics of those from the protons in nonaromatic alkene moiety, implying the change of pyridine ring mainly through nucleophilic addition and subsequent oxidation under the UV light irradiation.[41]

The MOF ZJU-56−0.20 retains its original crystal structure after the UV light irradiation, as shown in the PXRD pattern (Figure S6). This suggests that the UV light induced reactions do not destroy the backbone of the photoactive linker. After the photochemical reaction, charged nitrogen atoms in the pyridine rings turn neutral and the resultant amino groups serve as donors, leading to the formation of A−π−D−π−A π-conjugation, a typical structure of two-photon excited fluorescent molecules (Figure S9b). It is expected that the introduction of the donor moiety of the amino group will narrow the energy gap between π and π* states. Indeed, Figure S10 shows the emergence of a red-shifted absorption band in UV−vis spectrum of L1 solution after the treatment of UV laser, indicating the formation of new substances with a lower π−π* transition energy.

Processing of materials through two-photon effects offers a powerful tool to induce photochemical reactions (polymerization in most cases) and to generate 3D patterns/structures in high spatial precision, so the resulting 3D fluorescence structure can be readily imaged by the multiphoton fluorescence microscopy.[33,34] To utilize the two-photon effects of the photoactive linker for direct pattern writing, the two-photon induced photochemical response of the linker L1 in ZJU-56−0.20 was investigated using a confocal laser scanning microscope equipped with a tunable femtosecond laser. As shown in Figure 2c−e, a square region within a MOF crystal was scanned and irradiated by a 710 nm laser, whose photon energy is half of the UV laser at 355 nm in which the crystals absorb in the one-photon mode (Figure S10). Irradiated by femtosecond laser, the single crystal retained its morphology without any observable cracks and its fluorescence spectra were simultaneously recorded by the confocal microscope. The fluorescence spectra reveal that the emission band around 550 nm is gradually enhanced, similar to the response to UV light illumination (Figures 2 and S11).

Because the ultrahigh instantaneous energy density of femtosecond laser may yield unexpected heat effect and thus possibly induce the chemical reactions, we need to exclude such a possibility. To do this, another laser wavelength of 900 nm (similar power) was utilized as a reference. As shown in Figure 2d,e, the exposed region does not exhibit any fluorescence change during the 900 nm laser irradiation, and no clear fluorescent square is left there. The strong wavelength dependence for fluorescence change is consistent with the Z-scan data of the linker L1 (Figure S12), indicating that the photochemical process and fluorescence change are indeed attributed to two-photon absorption and excited state involved reaction. As mentioned above, a 710 nm laser can both induce the photochemical reaction and emission around 550 nm.
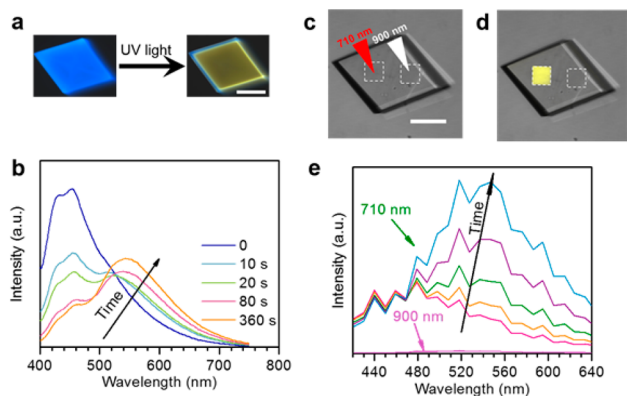
However, to image the recorded pattern, the laser at this wavelength is not suitable because it would induce reaction in the unaddressed area. The laser at 900 nm, which cannot initiate photochemical reactions, is able to excite the written areas, generating strong two-photon excited fluorescence (corresponding to 450 nm of one-photon excitation), as shown in the log−log scale plot in Figure S13.[45] On the basis of these nonlinear optical properties of **ZJU-56−0.20**, we can *write* and *read* fluorescent patterns fully through the two-photon processes with the laser at 710 and 900 nm, respectively.

Because of the unique two-photon response, a two-dimensional (2D) code fluorescent pattern (representing Zhejiang University) consisting of 25 × 25 primary square blocks (Figure S14) was chosen to demonstrate the ability to create multiple layered or 3D patterns into the MOF through two-photon processes. Two layers of the 2D code pattern with a depth interval of 12 μm were prepared inside the MOF crystal (see experimental details in the SI). Imaged with two-photon excited fluorescence, Figure 3a,b,d shows the top and lateral
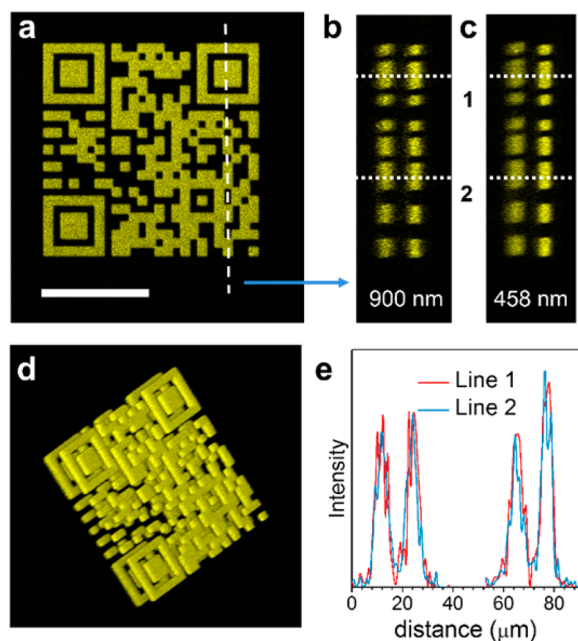

Figure 3. (a) Top view of two-photon excited fluorescent image of a 2D code stack. Scale bar, 25 μm. (b) Reconstructed lateral image along the indicated line in panel a. (c) Lateral view imaged by using one-photon fluorescence. (d) Three-dimensional reconstructed image of the stacked 2D code pattern. (e) Intensity profiles of the fluorescent codes along Lines 1 and 2 in panels b and c, respectively.

views, and the 3D reconstructed image of the two layers, respectively. As shown in Figure 3b,c,e, the two-photon excited fluorescence of both layers is similar, whereas the below pattern imaged with one-photon fluorescence (excited at 458 nm) is a little dimmer than the upper one. This result shows the superiority of two-photon imaging for a multilayered structure or deep samples.

The thickness of each layer is around 5 μm according to both lateral view and intensity profile of fluorescence (Figure 3b,e), indicating the depth resolution is about 5 μm. The lateral resolution is around 2 μm, which can be further improved. As shown in Figure S15, for example, a 25 × 25 μm^2 2D code with feature size of 1 × 1 μm^2 exhibits high quality and can be

recognized correctly. In this configuration of optical setup, the voxel size reaches a high resolution around 1 × 1 × 5 μm^3. Because of the irreversible photochemical process, the fluorescent pattern is much more stable than those reported[46] and does not show much decay even after 30 days (Figure S16). This kind of 3D two-photon excited fluorescence pattern may find usage in 3D optical storage.[34,46]

In summary, we developed a two-photon responsive MOF crystal **ZJU-56−0.20**, which shows significant red-shift change in two-photon excited fluorescence, ascribed to the photochemical reaction of the zwitterionic organic linkers, under the femtosecond laser. The nonlinear optical nature allows for two-photon patterning and imaging in high-resolution (1 × 1 × 5 μm^3) 3D structure. The approach of introducing nonlinear optical linkers into MOFs for 3D patterning and two-photon imaging will enable MOFs to be useful materials for sensor arrays and data storage media.

■ ASSOCIATED CONTENT

Ⓢ Supporting Information

Synthetic procedure, characterization and properties of MOFs, crystallographic data (CIF files), experimental details of two-photon patterning and imaging, the micrographs, and the spectral evidence of photochemical reaction. This material is available free of charge via the Internet at http://pubs.acs.org.

■ AUTHOR INFORMATION

Corresponding Authors
*banglin.chen@utsa.edu
*gdqian@zju.edu.cn

Author Contributions
[||]These authors contributed equally to this work.

Notes
The authors declare no competing financial interest.

■ ACKNOWLEDGMENTS

■ REFERENCES

(1) Furukawa, H.; Cordova, K. E.; O'Keeffe, M.; Yaghi, O. M. *Science* **2013**, *341*, 1230444.

(2) Foo, M. L.; Matsuda, R.; Kitagawa, S. *Chem. Mater.* **2014**, *26*, 310−322.

(3) Qiu, S.; Xue, M.; Zhu, G. *Chem. Soc. Rev.* **2014**, *43*, 6116−6140.

(4) Xiang, S.; He, Y.; Zhang, Z.; Wu, H.; Zhou, W.; Krishna, R.; Chen, B. *Nat. Commun.* **2012**, *3*, 954.

(5) Morris, R. E.; Bu, X. *Nat. Chem.* **2010**, *2*, 353−361.

(6) Yoon, M.; Srirambalaji, R.; Kim, K. *Chem. Rev.* **2011**, *112*, 1196−1231.

(7) Kreno, L. E.; Leong, K.; Farha, O. K.; Allendorf, M.; Van Duyne, R. P.; Hupp, J. T. *Chem. Rev.* **2012**, *112*, 1105−1125.

(8) Hu, Z.; Deibert, B. J.; Li, J. *Chem. Soc. Rev.* **2014**, *43*, 5815−5840.

(9) An, J.; Shade, C. M.; Chengelis-Czegan, D. A.; Petoud, S.; Rosi, N. L. *J. Am. Chem. Soc.* **2011**, *133*, 1220−1223.

(10) Talin, A. A.; Centrone, A.; Ford, A. C.; Foster, M. E.; Stavila, V.; Haney, P.; Kinney, R. A.; Szalai, V.; El Gabaly, F.; Yoon, H. P.; Léonard, F.; Allendorf, M. D. *Science* **2014**, *343*, 66−69.

(11) Wang, C.; Zhang, T.; Lin, W. *Chem. Rev.* **2012**, *112*, 1084−1104.

(12) Yu, J.; Cui, Y.; Xu, H.; Yang, Y.; Wang, Z.; Chen, B.; Qian, G. *Nat. Commun.* **2013**, *4*, 2719.

(13) Wiers, B. M.; Foo, M.-L.; Balsara, N. P.; Long, J. R. *J. Am. Chem. Soc.* **2011**, *133*, 14522−14525.

(14) Shimizu, G. K. H.; Taylor, J. M.; Kim, S. *Science* **2013**, *341*, 354−355.

(15) Sadakiyo, M.; Kasai, H.; Kato, K.; Takata, M.; Yamauchi, M. *J. Am. Chem. Soc.* **2014**, *136*, 1702−5.

(16) Li, S.-L.; Xu, Q. *Energy Environ. Sci.* **2013**, *6*, 1656−1683.

(17) Mukhopadhyay, R. D.; Praveen, V. K.; Ajayaghosh, A. *Mater. Horiz.* **2014**, *1*, 572−576.

(18) Park, J.; Yuan, D.; Pham, K. T.; Li, J.-R.; Yakovenko, A.; Zhou, H.-C. *J. Am. Chem. Soc.* **2011**, *134*, 99−102.

(19) Yanai, N.; Uemura, T.; Inoue, M.; Matsuda, R.; Fukushima, T.; Tsujimoto, M.; Isoda, S.; Kitagawa, S. *J. Am. Chem. Soc.* **2012**, *134*, 4501−4504.

(20) Lyndon, R.; Konstas, K.; Ladewig, B. P.; Southon, P. D.; Kepert, P. C. J.; Hill, M. R. *Angew. Chem., Int. Ed.* **2013**, *52*, 3695−3698.

(21) Luo, F.; Fan, C. B.; Luo, M. B.; Wu, X. L.; Zhu, Y.; Pu, S. Z.; Xu, W.-Y.; Guo, G.-C. *Angew. Chem., Int. Ed.* **2014**, *53*, 9298−9301.

(22) Tanabe, K. K.; Allen, C. A.; Cohen, S. M. *Angew. Chem., Int. Ed.* **2010**, *49*, 9730−9733.

(23) Allen, C. A.; Cohen, S. M. *J. Mater. Chem.* **2012**, *22*, 10188−10194.

(24) Sun, J.-K.; Cai, L.-X.; Chen, Y.-J.; Li, Z.-H.; Zhang, J. *Chem. Commun.* **2011**, *47*, 6870−6872.

(25) Williams, D. E.; Rietman, J. A.; Maier, J. M.; Tan, R.; Greytak, A. B.; Smith, M. D.; Krause, J. A.; Shustova, N. B. *J. Am. Chem. Soc.* **2014**, *136*, 11886−11889.

(26) Brown, J. W.; Henderson, B. L.; Kiesz, M. D.; Whalley, A. C.; Morris, W.; Grunder, S.; Deng, H.; Furukawa, H.; Zink, J. I.; Stoddart, J. F.; Yaghi, O. M. *Chem. Sci.* **2013**, *4*, 2858−2864.

(27) Patel, D. G.; Walton, I. M.; Cox, J. M.; Gleason, C. J.; Butzer, D. R.; Benedict, J. B. *Chem. Commun.* **2014**, *50*, 2653−2656.

(28) Heinke, L.; Cakici, M.; Dommaschk, M.; Grosjean, S.; Herges, R.; Bräse, S.; Wöll, C. *ACS Nano* **2014**, *8*, 1463−1467.

(29) Han, S.; Wei, Y.; Valente, C.; Forgan, R. S.; Gassensmith, J. J.; Smaldone, R. A.; Nakanishi, H.; Coskun, A.; Stoddart, J. F.; Grzybowski, B. A. *Angew. Chem., Int. Ed.* **2011**, *50*, 276−279.

(30) Ameloot, R.; Roeffaers, M. B. J.; De Cremer, G.; Vermoortele, F.; Hofkens, J.; Sels, B. F.; De Vos, D. E. *Adv. Mater.* **2011**, *23*, 1788−1791.

(31) Rumi, M.; Barlow, S.; Wang, J.; Perry, J. W.; Marder, S. R. Two-Photon Absorbing Materials and Two-Photon-Induced Chemistry. In *Photoresponsive Polymers I*; Marder, S. R., Lee, K.-S., Eds.; Springer: Berlin, Germany, 2008; Vol. *213*, pp 1−95.

(32) LaFratta, C. N.; Fourkas, J. T.; Baldacchini, T.; Farrer, R. A. *Angew. Chem., Int. Ed.* **2007**, *46*, 6238−6258.

(33) Helmchen, F.; Denk, W. *Nat. Methods* **2005**, *2*, 932−940.

(34) Lott, J.; Ryan, C.; Valle, B.; Johnson, J. R.; Schiraldi, D. A.; Shan, J.; Singer, K. D.; Weder, C. *Adv. Mater.* **2011**, *23*, 2425−2429.

(35) Kawata, S.; Sun, H.-B.; Tanaka, T.; Takada, K. *Nature* **2001**, *412*, 697−698.

(36) Zhou, W.; Kuebler, S. M.; Braun, K. L.; Yu, T.; Cammack, J. K.; Ober, C. K.; Perry, J. W.; Marder, S. R. *Science* **2002**, *296*, 1106−1109.

(37) Olson, C. E.; Previte, M. J. R.; Fourkas, J. T. *Nat. Mater.* **2002**, *1*, 225−228.

(38) He, T. C.; Chen, R.; Lim, Z. B.; Rajwar, D.; Ma, L.; Wang, Y.; Gao, Y.; Grimsdale, A. C.; Sun, H. D. *Adv. Opt. Mater.* **2014**, *2*, 40−47.

(39) He, T. C.; Gao, Y.; Chen, R.; Ma, L.; Rajwar, D.; Wang, Y.; Grimsdale, A. C.; Sun, H. D. *Macromolecules* **2014**, *47*, 1316−1324.

(40) Deng, H.; Doonan, C. J.; Furukawa, H.; Ferreira, R. B.; Towne, J.; Knobler, C. B.; Wang, B.; Yaghi, O. M. *Science* **2010**, *327*, 846−850.

(41) Görner, H.; Miskolczy, Z.; Megyesi, M.; Biczók, L. *Photochem. Photobiol.* **2011**, *87*, 1315−1320.

(42) Zhao, C. F.; He, G. S.; Bhawalkar, J. D.; Park, C. K.; Prasad, P. N. *Chem. Mater.* **1995**, *7*, 1979−1983.

(43) Rao, X.; Cai, J.; Yu, J.; He, Y.; Wu, C.; Zhou, W.; Yildirim, T.; Chen, B.; Qian, G. *Chem. Commun.* **2013**, *49*, 6719−6721.

(44) O'Keeffe, M.; Yaghi, O. M. *Chem. Rev.* **2012**, *112*, 675−702.

(45) Wang, Y.; Ta, V. D.; Gao, Y.; He, T. C.; Chen, R.; Mutlugun, E.; Demir, H. V.; Sun, H. D. *Adv. Mater.* **2014**, *26*, 2954−2961.

(46) Parthenopoulos, D. A.; Rentzepis, P. M. *Science* **1989**, *245*, 843−845.